STRUCTURE OF A FIXED AND A FLUIDIZED BED OF GRANULAR MATERIAL NEAR AN IMMERSED SURFACE (WALL)

V. N. Korolev, N. I. Syromyatnikov, and E. M. Tolmachev

UDC 532.546

The porosity of a fixed and a fluidized bed near a wall are determined experimentally by means of x-radioscopy and the results are presented.

It is well known [1-3] that the structure and, specifically, the porosity of a fixed and a fluidized granular bed is different adjacent to and at some distance from an immersed surface or a boundary wall. In order to analyze correctly the effect of the gaseous and the solid phase on the process of heat and mass transfer between an immersed body and the bed, therefore, it is necessary to know the porosity distribution at the surface across which the heat transfer occurs.

We present here the results of an experimental study concerning the local porosity distribution in a fixed and a fluidized bed near an immersed body, these results having been obtained by layerwise x-radioscopy of the granular bed.

The test apparatus is shown schematically in Fig. 1. A fluidized bed was built up in compartment 1 100 × 100 mm square and 400 mm high, with a mesh having a 2% active cross section (diameter of holes 0.63 mm). In order to ensure a uniform gas distribution, a foam sheet was placed on top of the mesh. In the middle of the apparatus a polished plate 2 70 × 80 mm large and 10 mm thick was rigidly mounted. Its lower surface with rounded edges was 10 mm away from the mesh. To permit the determination of the porosity of the fluidized bed directly at the plate surface – except for the material between the apparatus walls and the sides of the plate – a special duct 3 was provided for the x-ray beam. This duct had a rectangular cross section 5 × 13 mm, i.e., was sufficiently large for measuring the porosity of a layer 5 mm away from the plate surface.

An x-ray beam 0.1 mm wide and 10 mm high was transmitted into the bed from a URS-50-1M machine. A beam of such dimensions was shaped by means of a slotted diaphragm 4 mounted in the exit window of the x-ray tube 5 and before a Geiger counter 6. The intensity of radiation passing through the bed was recorded by this counter and subsequently read out by means of radio-engineering devices 7. The radiation intensity was measured by the integrating method with a direct-indication instrument 8 calibrated in pulses per second, and was also read on the strip chart of an automatic potentiometer device 9 the pen deflection of which was proportional to the count rate recorded by the integrating instrument.

Such a narrow beam made it possible to determine the local porosity ε_{loc} (the porosity in the section through which the x-ray beam passed) or the translucence of a bed section 50 mm above the mesh. The distance between the plate surface and the x-ray beam was checked with a 0.01 mm precision.

The basis of the x-radioscopic method of determining the bed porosity is that, on passing through the bed, the beam undergoes a change in intensity dependent on the density of the medium. Assuming that narrowly collimated monochromatic x-rays which pass through a granular layer are absorbed according to Bouguer's law [4], we write

$$I = I_0 \exp\left(-\sum_i \mu_i d_i\right). \tag{1}$$

In this case the absorbing layer consists of two apparatus walls, each δ_w thick, and the mechanical mixture of particles and air; therefore

S. M. Kirov Ural Polytechnical Institute, Sverdlovsk. Translated from Inzhenerno-Fizicheskii Zhurnal, Vol. 21, No. 6, pp. 973-978, December, 1971. Original article submitted February 16, 1971.

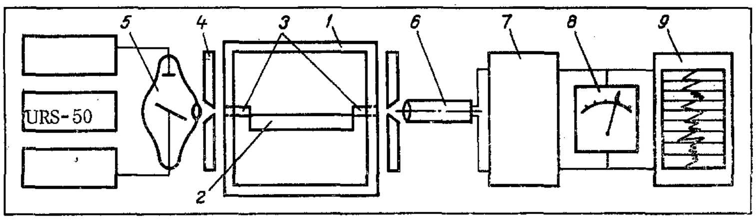

Fig. 1. Schematic diagram of the test apparatus.

$$\sum_i \mu_i d_i = 2\mu_w d_w + \mu_1 d_1, \tag{2}$$

where

$$\mu_1 = \mu_b(1-\varepsilon) + \mu_c\varepsilon. \tag{3}$$

Inserting (3) into (2) and then into (1) yields, with the background radiation taken into account,

$$I - I_b = (I_0 - I_b)\exp\{-2\mu_w d_w - [\mu_p(1-\varepsilon) + \mu_a\varepsilon]\, d_1\}. \tag{4}$$

Let

$$(I_0 - I_b)\exp(-2\mu_w d_w) = I_1 - I_b. \tag{5}$$

then

$$I - I_b = (I_1 - I_b)\exp\{-[\mu_q(1-\varepsilon) + \mu_a\varepsilon]\, d_1\}. \tag{6}$$

From (3) we have

$$\varepsilon = \frac{\mu_p - \mu_1}{\mu_p - \mu_a}.$$

Disregarding μ_a (of the order of 10^{-4} cm^{-1}), we have

$$\varepsilon = 1 - \frac{\mu_1}{\mu_p}. \tag{7}$$

Having found the value of μ_b from (6), we insert it into (7) and obtain

$$\varepsilon = 1 - \frac{1}{d_1\mu_p}\ln\frac{I_1 - I_b}{I - I_b}.$$

If we designate

$$\varepsilon = f\left(K\ln\frac{I_1 - I_b}{I - I_b}\right)$$

then

$$\frac{1}{d_1\mu_p} = K.$$

The linear dependence

$$\varepsilon = 1 - K\ln\frac{I_1 - I_b}{I - I_b} \tag{8}$$

obtained in semilogarithmic coordinates allows us to plot a graph calibrated at two points corresponding to the mean porosity of a fixed bed and to porosity 1.0 of a completely fluidized bed. From such a graph (a separate graph was plotted for each of the materials tested) we can determine the intermediate porosities. The mean porosity of a fixed bed is obtained by the Danton method [2].

Since the intensity of radiation passing through a fluidized bed varied with time, following variations in the local density of the medium, values for the intensity at a given distance from the plate surface averaged over 30 sec were taken for the calculation.

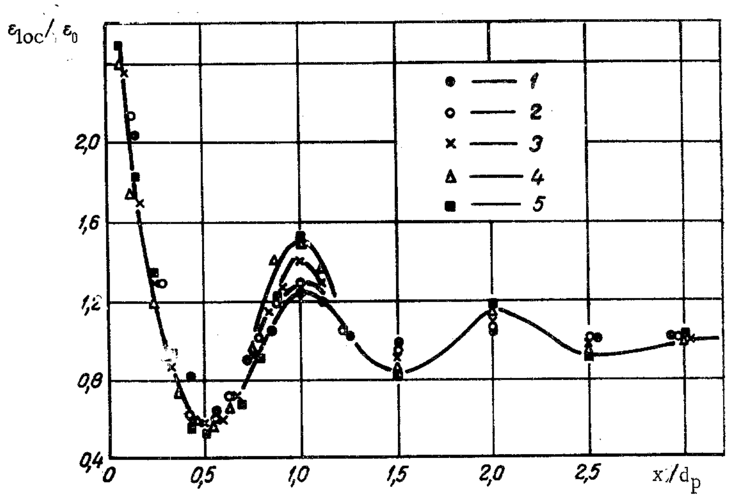

Fig. 2. Relative porosity $\varepsilon_{loc}/\varepsilon_0$ in a fixed bed of spherical particles at distance x/d_p from the wall: 1) $d_p = 0.72$ mm; 2) 0.80 mm; 3) 1.2 mm; 4) 1.74 mm; 5) 2.15 mm.

The maximum error in determining the local porosity by this procedure could be 8-10%.

The solid phases in these tests were tight fractions of spherical polystyrene granules 0.72, 0.82, 1.20, 1.74, 2.15 mm in diameter and chamotte particles of equivalent diameter 0.32, 0.48, 0.70, 0.85, 1.20 mm. The fluidizing agent was air at room temperature. The layer of charge was in all tests 85 mm high.

The test data on the local distributions of porosity (translucence) in a fixed bed of spherical particles near the walls referred to the mean porosity ε_0 are shown in Fig. 2.

According to the graph, the local porosity ε_{loc} is 1.0 at the wall, passes through a minimum at a distance of half a particle diameter from the wall, and reaches a maximum at a distance of one particle diameter from the wall. As a consequence of the sharp maximum ε_{loc} at $x/d_p = 1$, we may conclude that the packing of particles at the surface is cubic. Some differences between the curves of local porosity distribution for particles of different diameters in Fig. 2 can, apparently, be explained by the finite rather than zero width of the x-ray beam. Indeed, assuming a cubic packing of particles, it is not difficult to derive an expression for the minima of the curves at $x/d_p = 0.5$:

$$\varepsilon_{loc} = \varepsilon_1 + \frac{1}{2}(1 - \varepsilon_0)\left(\frac{\delta}{d_p}\right)^2. \tag{9}$$

By inserting the values of ε_1, ε_0, and δ for various d_p into (9), it may be verified that the calculated values of ε_{loc} differ from the measured values only slightly (within the test accuracy). In the case of an ideal packing of spherical particles over the entire bed volume, the expression for ε_{loc} becomes:

$$\varepsilon_{loc} = 1 - \frac{\pi}{6}\left[6\left(\frac{x}{d_p}\right)\left(1 - \frac{x}{d_p}\right) - \frac{1}{2}\left(\frac{\delta}{d_p}\right)^2\right] \tag{10}$$

for $0 \le x/d_p \le 1$ and it repeats periodically for the successive rows of particles.

According to the experimental evidence, however, the ordering effect of the wall on the packing of the particles diminishes with increasing distance from the wall and at $x/d_p < 3$ the packing becomes almost random. Equation (10) may also be used to estimate the packing in the second row from the surface. Thus, when the packing of the first row is close cubic, particles in the second row may penetrate into the first row to a distance $x/d_p = 0.857$. Here the calculated value of ε_{loc} (0.617) is higher than that indicated by test (~0.480), which means that the packing of particles in the first row is not close (for a fixed bed the value of ε_{loc} was measured after the sedimentation of a suspended layer).

The local porosity in a bed with chamotte particles of random shapes, in contrast to the case of spherical particles, varied almost smoothly from 1.0 at the surface to ε_0 at a distance of approximately two particle diameters.

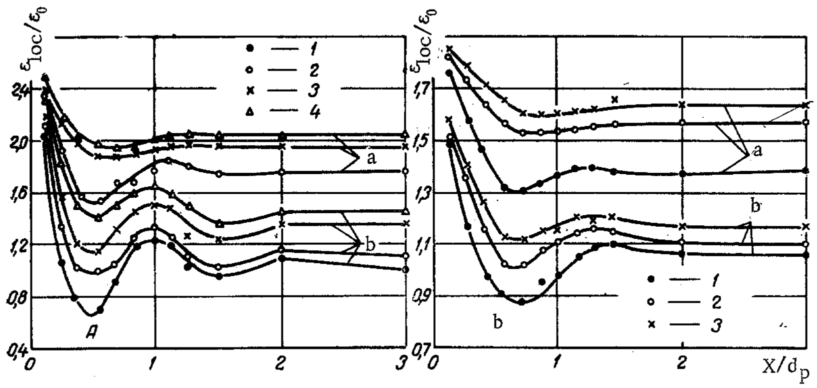

Fig. 3. Relative porosity $\varepsilon_{loc}/\varepsilon_0$ of a fluidized bed with spherical particles (A) and with particles of random shape (B) as a function of the distance x/d_p from the plate (a) and from the apparatus wall (b). For A: 1) W = 1; 2) 2; 3) 5; 4) 8, for B: 1) W = 1; 2) 2; 3) 3.

The test data on local porosity distribution in a fluidized bed – referred to the mean porosity of a fixed bed – are shown in Fig. 3 for spherical 0.72 mm polystyrene particles and chamotte particles with an equivalent diameter of 0.70 mm, near a plate immersed in the bed and near the apparatus wall.

As the graph indicates, under the same conditions of fluidization the value of ε_{loc} is larger near the surface of the plate immersed in the bed than at the side surface of the apparatus. This, evidently, causes the difference noted by many authors [5] between the heat-transfer coefficients for those surfaces. Analogous results on the local porosity distribution in a fluidized bed near a plate and near an apparatus wall have also been obtained with other test materials.

NOTATION

I_0	is the intensity of the incident radiation;
I	is the intensity of the radiation passing through a layer of the bed;
I_1	is the intensity of the radiation after passage through a layer;
μ_l, μ_p, μ_a, μ_w	are the linear coefficient of x-ray attenuation by the layer, by the particles, by the air, and by the wall, respectively;
d_l	is the thickness of the layer;
d_p	is the particle diameter;
x	is the distance from the plate (wall);
δ	is the x-ray beam width;
ε_1	is the minimum local porosity (translucence) with a zero beam width;
W	is the fluidization number.

LITERATURE CITED

1. M. Kimura, K. Nono, and T. Kaneda, Chem. Engr. Japan, 19, 397 (1955).
2. M. É. Aerov and O. M. Todes, Hydraulic and Thermal Operating Principles of Fixed-Bed and Fluidized-Bed Apparatus with Granular Material [in Russian], Khimiya, Leningrad (1968).
3. V. N. Korolev and N. I. Syromyatnikov, Zh. VKhO im. D. I. Mendeleeva, 15, 585 (1970).
4. L. K. Tatotchenko, Radioactive Isotopes and Instrument Design [in Russian], Atomizdat (1960).
5. N. I. Gel'perin, V. G. Ainshtein, and V. B. Kvasha, Principles of Fluidized-Bed Technology [in Russian], Khimiya (1967).